

Cite this: *Dalton Trans.*, 2017, **46**, 9833

Calix[4]arene-fused phospholes†

Fethi Elaieb, ^a David Sémeril, ^{*a} Dominique Matt, ^{*a} Michel Pfeffer, ^b Pierre-Antoine Bouit, ^c Muriel Hissler, ^{*c} Christophe Gourlaouen ^d and Jack Harrowfield ^e

An upper rim, *o*-(diphenylphosphinyl)phenyl-substituted calix[4]arene has been prepared and its coordinative properties investigated. When heated in the presence of palladium, the new biarylphosphine undergoes conversion into two diastereomeric, calixarene-fused phospholes. In both, the P lone pair adopts a fixed orientation with respect to the calixarene core. The more hindered phosphole (**8**), *i.e.* the one with the *endo*-oriented lone pair (cone angle 150°–175°), forms complexes having their metal centre positioned very near the calixarene unit but outside the cavity, thus inducing an unusual chemical shift of one of the methylenic ArCH₂Ar protons owing to interactions with the metal centre. As expected for dibenzophospholes, the complex [Rh(acac)(CO)·**8**], when combined with one equivalent of free **8**, efficiently catalyses the hydroformylation of styrene, the catalytic system displaying high regioselectivity in favour of the branched aldehyde (*b/l* ratio up to 30). The optical and redox properties of the derivatives have also been investigated.

Received 26th May 2017,
Accepted 21st June 2017

DOI: 10.1039/c7dt01899a

rsc.li/dalton

Introduction

Cavity-shaped molecules equipped with P(III) donor atoms have attracted increasing attention in the last two decades due to their successful applications in transition metal catalysis.¹ Notably, a number of publications have shown that the presence of a conical cavity fixed near a catalytic centre may drastically influence the outcome of carbon–carbon bond forming reactions in terms of both activity and selectivity.² A current challenge in this chemistry concerns the synthesis of calix[4]arenes in the so-called *cone* conformation substituted by a P(III) atom having its lone pair permanently located on the *endo*-face of the cavity. Conical molecules with this feature are

expected to result in complexes with a highly crowded metal environment, if not with a metal centre embedded in the cavity.^{2*i,j*,3} A number of cone-calix[4]arenes bearing a PR₂ group as an upper rim substituent have already been reported, but in none of them does the P doublet adopt a fixed *endo*-orientation, which is due to the rotational freedom of the PR₂ moiety about the corresponding P–C_{calix} bond.⁴ Blocking the mobility of *endo*-P-conformers would certainly increase the time-averaged bulkiness of the corresponding ligand.

Here, we describe the synthesis of a calix[4]arene-based biarylphosphine and its catalytic conversion into two calix[4]arene-fused phospholes, with one of them having its P lone pair rigidly positioned on the concave side of the cavity. The coordinative properties of the latter towards Pd(II), Au(I) and Rh(I) were investigated. Both ligands constitute the first example of unsymmetrical dibenzophospholes sharing one of their benzo rings with that of a calix[4]arene receptor.⁵ Note that another calixarene linked to a phosphole unit has been reported recently, however with the phosphole ring remote from the cavity core.⁶

Results and discussion

Synthesis and coordinative properties of a phosphole precursor

Our strategy for preparing a calix[4]arene merged with a phosphole ring is based on a recent paper by Chatani *et al.* where it was shown that biarylphosphines of the general formula Ph₂P

^aLaboratoire de Chimie Inorganique Moléculaire et Catalyse, Institut de Chimie (UMR 7177 CNRS), Université de Strasbourg, 1 rue Blaise Pascal, F-67008 Strasbourg Cedex, France. E-mail: dmatt@unistra.fr, dsemeril@unistra.fr

^bLaboratoire de Chimie et Systématique Organométallique, Institut de Chimie (UMR 7177 CNRS), Université de Strasbourg, 1 rue Blaise Pascal, F-67008 Strasbourg Cedex, France

^cInstitut des Sciences Chimiques de Rennes (UMR 6226 CNRS), Université de Rennes 1, Groupe "Phosphore et Matériaux Moléculaires", Campus de Beaulieu, 263, avenue du Général Leclerc, F-35042 Rennes Cedex, France.

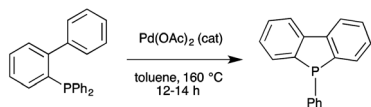
E-mail: muriel.hissler@univ-rennes1.fr

^dLaboratoire de Chimie Quantique, Institut de Chimie (UMR 7177 CNRS), Université de Strasbourg, 1 rue Blaise Pascal, F-67008 Strasbourg, France

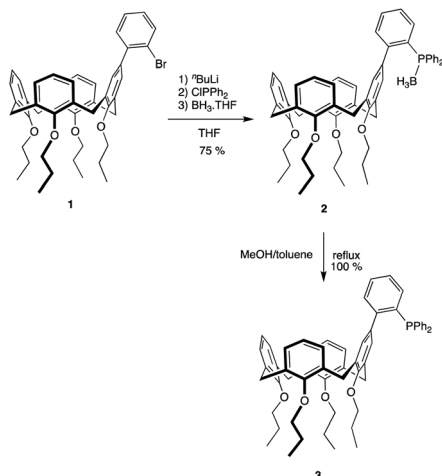
^eInstitut de Science et Ingénierie Supramoléculaire (ISIS), UMR 7606 CNRS,

Université de Strasbourg, 8 rue Gaspard Monge, 67083 Strasbourg cedex, France

†Electronic supplementary information (ESI) available. CCDC 1455997 and 1545340–1545342. For ESI and crystallographic data in CIF or other electronic format see DOI: 10.1039/c7dt01899a



Scheme 1 Chatani's method for the catalytic synthesis of a phenyl-phosphole.

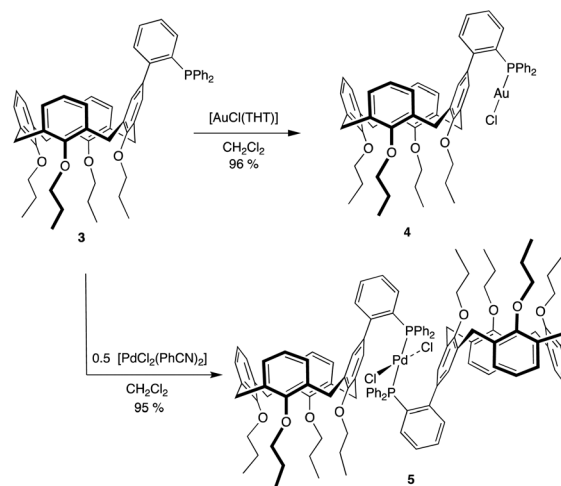


Scheme 2 Synthesis of phosphine **3**.

(*o*-Ar-C₆H₄) may, in the presence of [Pd(OAc)₂], undergo catalytic conversion into a dibenzophosphole (Scheme 1).⁷ We anticipated that applying this methodology to the (unreported) biaryl-phosphine **3** (Scheme 2), in which the P-remote arene ring is part of a conical calix[4]arene skeleton, would result in a calixarene-fused phosphole.

The synthesis of precursor **3** was performed in two steps, as shown in Scheme 2. Thus, reaction of the bromoaryl-substituted calixarene **1**⁸ with *n*-BuLi followed by the addition of PPh₂Cl to the resulting mixture and subsequent treatment with BH₃·THF gave the phosphine borane adduct **2** in 75% yield. Deprotection with MeOH/toluene gave **3** quantitatively. The ³¹P NMR spectrum of **3** shows a single resonance at -12.4 ppm (*cf.* δ_P (PPh₃) = -4 ppm; δ_P [Ph₂P(*o*-Ph-C₆H₄)] = -11.9 ppm). The corresponding ¹H NMR spectrum, which exhibits two distinct AB patterns for the bridging ArCH₂Ar groups (both with AB separations of *ca.* 1.3 ppm), is fully consistent with a calix[4]arene in the cone conformation.⁹

The coordinative properties of **3** towards Au(I) and Pd(II) were investigated. Thus, reaction of **3** with [AuCl(THT)] gave **4** quantitatively (Scheme 3). Complex **4** was characterised by ¹H-, ¹³C-, and ³¹P-NMR spectroscopy (see the Experimental section) as well as using a single crystal X-ray diffraction study (Fig. 1), which revealed a typical “pinched cone” structure of the calixarene core in the solid state. The P–Au–Cl rod is located outside the calixarene cavity with the gold atom lying above one of the C–C bonds of the phosphinated phenol ring. The values of the shortest Au⋯C_{calix} separations, 3.278 Å and 3.373 Å, are indicative of weak η²-Au-arene interactions,



Scheme 3 Complexes obtained from phosphine **3**.

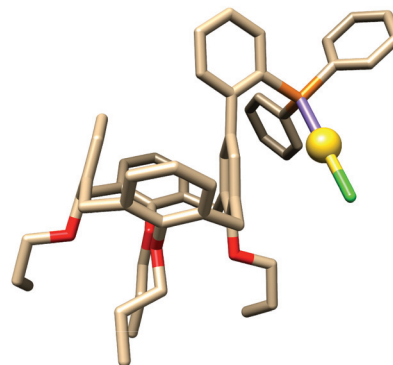


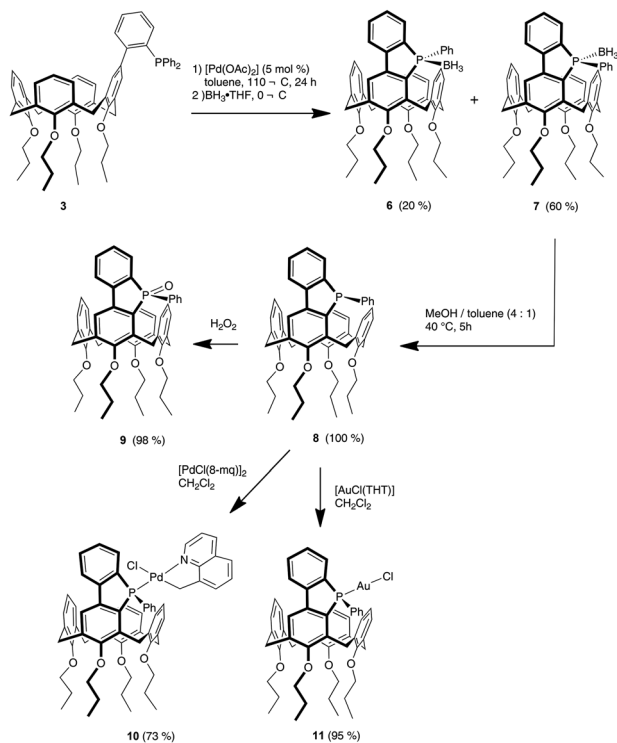
Fig. 1 Molecular structure of **4**.

similar to those recently proposed by Echavarren *et al.* for the biarylphosphine complex [AuCl(Cy₂P(*o*-Ph-C₆H₄))].¹⁰

Reaction of **3** with 0.5 equiv. of [PdCl₂(PhCN)₂] in CH₂Cl₂ (Scheme 3) resulted selectively in *trans*-[PdCl₂·**3**]₂ (**5**). Spectroscopic data are fully consistent with the presumed structure of this complex (see the Experimental part). In particular, assignment of the *trans* stereochemistry was made by comparing the chemical shift of the P atom (δ_P = 22.3 ppm) with that measured for a related complex, *trans*-[PdCl₂{Ph₂P(*o*-Ph-C₆H₄)}₂] (δ_P = 22.3 ppm).¹¹ A preliminary X-ray study confirmed this assignment.

Catalytic conversion of phosphine **3** to the calix-fused phosphole **8**

Thermal treatment of a solution of **3** in toluene for 24 h in the presence of [Pd(OAc)₂] (5 mol%) and subsequent reaction with BH₃·THF afforded the two isomeric phosphole-borane adducts **6** (20%) and **7** (60%), which were separated by column chromatography (Scheme 4). Both compounds possess a stereogenic phosphorus atom, one bearing an *exo*- and the other an *endo*-oriented BH₃ moiety (here the terms *exo* and *endo* stand,



Scheme 4 Synthesis of calix-fused phosphole **8** and its derivatives **9**, **10** and **11**.

respectively, for a BH_3 moiety directed towards the convex or concave part of the cavity). Owing to the C_1 molecular symmetry, the bridging methylene groups of each calixarene appear as four distinct AB patterns in the corresponding ^1H NMR spectra.

As generally observed for $\text{P}(\text{III})$ -borane adducts, the ^{31}P NMR spectra of **6** and **7** each display a rather broad signal due to ^{31}P - ^{11}B coupling. Remarkably, while all aromatic protons of **7** are to be found in the range 7.92–6.04 ppm, the ^1H NMR spectrum of the *exo*-adduct **6** displays signals at higher field for three aromatic protons (5.87 (d), 5.65 (t) and 4.71 (d)), probably owing to a ring current effect exerted by the *endo*-oriented PPh ring on the three H atoms of the phenoxy ring closest to the phosphorus atom. Note that both calixarenes are inherently chiral, and therefore they must each form a racemic mixture. It is also important to note that, as shown previously,¹² when the above reaction was performed with analogues of **3** bearing either a PCy_2 or a P^iPr_2 substituent (instead of PPh_2), no phosphole formation occurred.

Phosphole-borane deprotection was achieved only for *endo* adduct **7**. A very efficient deprotection method consisted of reacting a toluene solution of **7** with MeOH at 40 °C for 5 h (Scheme 4). After heating, the solution was evaporated to dryness, affording pure **8** quantitatively. The phosphorus atom of **8** gives a peak at -11.5 ppm in the ^{31}P NMR spectrum. Prolonged heating of a CDCl_3 solution of **8** at temperatures above 45 °C induced very slow formation of the isomer resulting from pyramidal inversion at phosphorus (appearance of a

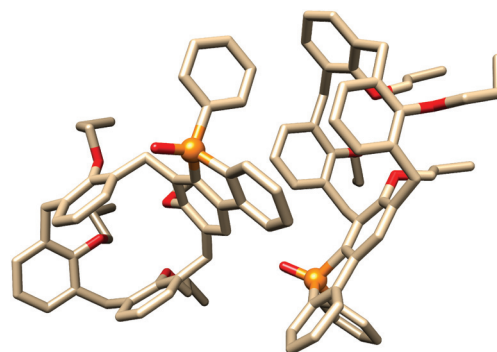


Fig. 2 Solid state structure of **9**. The two conformers seen in the solid form a kryptoracemate.¹⁶ The dihedral angles between the facing phenoxy rings are 14.3° and 79.1°, respectively, in conformer A, and 5.9° and 74.6°, respectively, in conformer B.

signal at -13.9 ppm). The ultimate proof of the *endo* stereochemistry of **7** came from an X-ray diffraction study (Fig. 2) performed on the corresponding oxide **9**, which can be obtained by reacting **8** with H_2O_2 (Scheme 4). Determination of the Tolman cone angle of the phosphole-P based on the solid state data of **9** led to a value of *ca.* 150°. As shown in Fig. 2, in the solid state, the calixarene core of **9** adopts a typical “flattened cone” conformation in which two facing phenoxy rings are roughly parallel while the other two make an angle of *ca.* 75°. In fact, in solution the time-averaged cone angle of **8** is likely to be significantly higher than 150°, as conical calixarenes are known to undergo a “breathing motion” in which the facing phenoxy rings alternately come close together and then move away from each other (giving rise to the so-called flattened cone/flattened cone equilibrium^{1a}). Thus, a simulation with Spartan¹³ showed that the highest possible cone angle of **8** is 175°. For comparison, both 1,3,5-triphenylphosphole and PPh_3 have a cone angle of 145°.^{5c,14} Determination of the percentage buried volume of **8** using the SambVca tool¹⁵ led to a value of 35.0 (*vs.* 31.7 for PPh_3). The corresponding steric map (Fig. 3) clearly estab-

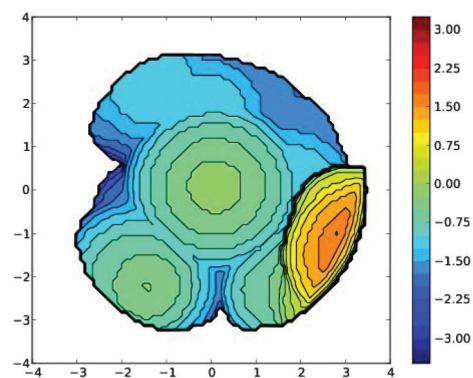


Fig. 3 Steric map of **8** (determined from the X-ray structure of **11**). View along the P-lone pair, taken as the z axis in the middle of the figure). The red-orange domain corresponds to the calixarene moiety. The coloured scale indicates the height on the z axis.

lished the proximity of the calixarenyl-P lone pair and the calixarene unit.

To obtain insight into its coordinative behaviour, phosphole **8** was reacted with the cyclopalladated complex $[\text{PdCl}(8\text{-mq})]_2$ (8-mqH = 8-methylquinoline). This reaction afforded complex **10** in 73% isolated yield. In the ^{31}P NMR spectrum, the phosphorus atom is observed at 25.7 ppm, a normal value for $[\text{PdCl}(8\text{-mq})(\text{phosphine})]$ complexes.¹⁷ In accord with the C_1 molecular symmetry, the Pd-bound CH_2 group of **10** appears as an ABX spectrum in the ^1H NMR spectrum, with $\delta_A = 3.12$ ppm and $\delta_B = 2.42$ ppm ($J(\text{BA}) = 14.5$ Hz; $^3J(\text{PA}) = 0$ Hz and $^3J(\text{PB}) = 7.5$ Hz). The PdCH^B signal at 2.42 ppm is shifted somewhat upfield when compared with those of other $[\text{PdCl}(8\text{-mq})(\text{phosphine})]$ complexes found in the literature (typical δ around 3.2 ppm).¹⁷ The observed shielding is likely to reflect the magnetic anisotropy created by the flat dibenzophospholyl unit located beneath one of the PdCH_2 atoms. This interpretation is consistent with the data inferred from the solid state structure of **10** (*vide infra*). An unusual feature which reflects the metal/cavity contiguity concerns the AB pattern of one of the four bridging ArCH_2Ar groups, the B signal of which has undergone a strong downfield shift upon complexation ($\delta_B = 4.52$ ppm, instead of an expected value of around 3.0 ppm), thus leading to an AB separation of only 0.17 ppm. The other three ArCH_2Ar signals show the normal pattern with AB separations of about 1.3 ppm, in accord with those usually observed for conical calix[4]arenes. In fact, owing to the fixed orientation of the P lone pair in **8**, complexation of the “PdCl(8-mq)” moiety positions the Pd–Cl bond close to one of the ArCH_2 groups, thereby allowing: (a) the metal-bound Cl atom to weakly interact with the equatorial CH atom; (b) the metal atom to create an anagostic $\text{CH}\cdots\text{Pd}$ bond, and (c) the phosphorus atom to give rise to a van der Waals interaction with the equatorial ArCH atom. All three interactions are compatible with the observed downfield shift. Note that anagostic bonds, which are electrostatic interactions in nature, are well documented in palladium chemistry.¹⁸

The structure of complex **10** was established by a single-crystal X-ray diffraction study (Fig. 4). The study confirmed that the P–Pd vector lies on the concave side of the calixarene and revealed that the metallacyclic unit lies out of the pinched

cavity. In the crystal, two molecules (A and B) are present, which display notable differences. In molecule A the quinolyl-inyl group lies as expected in the metal plane, while in B it is bent by *ca.* 36° towards the A molecule so as to enable π – π stacking interactions with the neighbouring quinolyl plane (the shortest intermolecular C \cdots C distances: 3.24 Å, 3.25 Å).

The study further confirmed the close proximity of both the Pd and Cl atoms to an equatorial ArCH_2Ar atom of the calixarene core. The corresponding $\text{Pd}\cdots\text{H}_{\text{eq}}$ (3.05 Å in A and 3.01 Å in B) and $\text{Cl}\cdots\text{H}_{\text{eq}}$ (3.0 Å in A and 3.45 Å in B) separations are compatible with the above postulated weak interactions, although at the upper limit for such interactions. However, due to the flexibility of the calixarene core, the time-averaged separations may be shorter in solution than those seen in the solid state. DFT optimisation starting from the X-ray structure led to a $\text{H}_{\text{eq}}\cdots\text{Cl}$ separation of 2.63 Å, a value that is fully consistent with a hydrogen bond (electrostatic interaction). The same calculation further established an electrostatic $\text{Pd}\cdots\text{H}_{\text{eq}}$ interaction (2.76 Å; see the ESI†), as well as a $\text{P}\cdots\text{H}_{\text{eq}}$ dispersion interaction (2.88 Å).

Finally, in accord with the observation of an upfield-shifted Pd–CH signal, in both molecules a CH atom sits in the shielding zone of the flat phospholyl unit (distance to the plane: 2.78 Å in A; 2.45 Å in B).

To determine whether the replacement of the “PdCl(8-mq)” moiety in **10** by a smaller metal fragment would modify the NMR signature of the ArCH_2 group closest to the metal, we prepared complex **11** (Scheme 4 and Fig. 6), which was obtained quantitatively by reacting **8** with $[\text{AuCl}(\text{THT})]$ (THT = tetrahydrothiophene). Its solid state structure was established using an X-ray diffraction study (Fig. 5). As for **10**, the ^1H NMR spectrum of **11** shows 4 different AB systems for the methylene bridges, three of which have their A and B parts separated by a Δ_{AB} value of *ca.* 1.3 ppm (see the Experimental part). The fourth ArCH_2 group displays a Δ_{AB} of 0.57 ppm, compared to 0.17 ppm in **10**. The smaller Δ_{AB} value found for **10** (*vs.* **11**) may reflect the $\text{M}\cdots\text{Cl}$ interaction occurring in this complex and its absence in **11**. The fact that the Δ_{AB} value in **11** still remains significantly smaller than 1.3 ppm could not be rationalised by DFT. Interestingly, these calculations revealed the existence of another favourable conformer, which possibly facilitates reversible dissociation of the AuCl unit (note that the methylene AB patterns of **11** are very similar to those of free phosphole **8**).

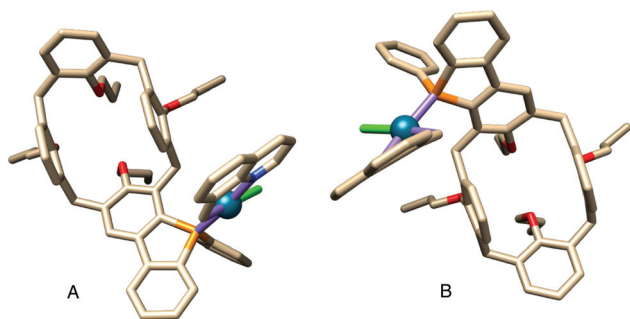


Fig. 4 Solid state structure of the phosphole palladium complex **10**, showing the two inequivalent molecules present in the unit cell.

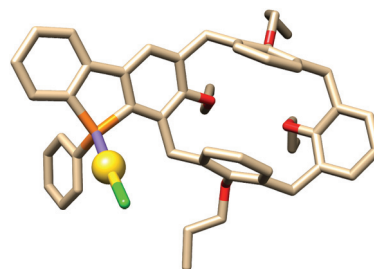


Fig. 5 Molecular structure of the gold phosphole complex **11**.

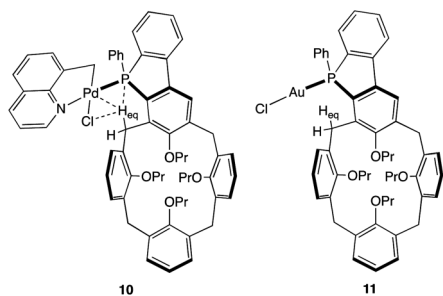
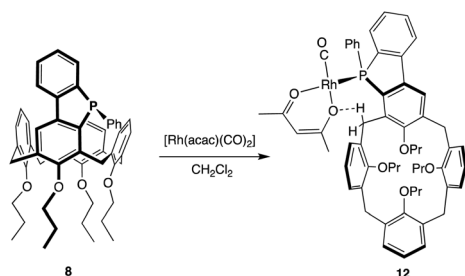


Fig. 6 Possible interactions (dashed lines) involving an equatorial ArCH atom in **10** and the formula of **11**.

Styrene hydroformylation with phosphole **8**

Dibenzo[*b,d*]phosphole **8** can be regarded as a triarylphosphine, and as such justifies its use in catalytic reactions.¹⁹ In order to assess **8** as a ligand for vinyl arenes hydroformylation, we prepared the mono-phosphole complex [Rh(acac)(CO)(**8**)] (**12**), which was obtained by reacting [Rh(acac)(CO)₂] with 1 equiv. of **8** (Scheme 5). Spectroscopic data are fully consistent with the proposed structure. Thus, for example, the IR spectrum of **12** shows a strong absorption band at 1975 cm⁻¹ for



Scheme 5 Synthesis of rhodium complex **12**.

the CO ligand and the ³¹P NMR spectrum shows a doublet at 56.0 ppm ($J(\text{PRh}) = 172 \text{ Hz}$) for the phosphorus atom. As for **10**, the ¹H NMR spectrum of **12** features four AB patterns for the methylene ArCH₂ groups, three of them with a Δ_{AB} value of *ca.* 1.3 ppm and the fourth with an AB separation of only 0.22 ppm. The existence of a tight AB pattern here may be attributed to a strong CH...O_{acac} interaction, as inferred from a DFT calculation. The latter calculation rules out an anagostic CH...Rh bond (although CH anagostic interactions with Rh have been reported²⁰).

Catalytic runs with **12** were carried out in toluene at 60 °C under a H₂/CO (1 : 1) pressure of 30 bar and with a Rh/styrene ratio of 1000 (Table 1). Using **12** alone as a catalyst resulted in a 69.0% styrene conversion after 7 h (Table 1, entry 1). As is usual for Rh/phosphine hydroformylation catalysts, adding one equivalent of free ligand to the complex induced a significant activity increase, the styrene conversion reaching then 81.7% after 7 h (Table 1, entry 2). The TOF determined after 1 h was 160 mol(styrene) mol(Rh)⁻¹ h⁻¹, compared to 75 mol(styrene) mol(Rh)⁻¹ h⁻¹ when using PPh₃ under the same conditions. We noted that the addition of a second equivalent of phosphole induced a slight decrease in activity with respect to the runs carried out with one equivalent of **8** (Table 1, entry 3). High regioselectivity in favour of the branched aldehyde (superior to those reported for other unsymmetrical benzo-phospholes¹⁹) was observed for each run, the branched/linear ratio amounting to 96.8 : 3.2 in the best case (Table 1, entry 3). In comparison, PPh₃ resulted in a *b/l* ratio of 93.5 : 6.5. Similar good performances were observed with the substrates 4-fluorostyrene and 4-^tBu-styrene (Table 1, entries 5 and 6). No hydrogenation products (ethylbenzene and 2-phenylpropanol) were detected in these experiments.

Photophysical and electrochemical properties of phosphole oxide **9** and gold complex **11**

The following studies were undertaken to quantify the influence of the calixarene moiety on the electronic properties of

Table 1 Rhodium-catalysed hydroformylation of vinyl arenes^a

Entry	R	Extra 8 (equiv./Rh)	Time (h)	Conversion ^b (%)	Aldehyde distribution ^b	
					<i>l</i> (%)	<i>b</i> (%)
1		0	7	69.0	5.0	95.0
2		1	7	81.7	4.8	95.2
3		2	7	46.7	3.2	96.8
4		1	22	100	5.8	94.2
5		1	22	100	3.7	96.3
6		1	22	100	5.4	94.6

^a Conditions: Complex **12** (2 μmol), **8**, vinyl arene (2 mmol), toluene/*n*-decane (20 mL/0.25 mL), P(CO/H₂) = 30 bar (CO/H₂, 1 : 1 v/v), 60 °C.

^b Determined by GC using decane as an internal standard.

Table 2 Optical and electrochemical data of **9** and **11**

	λ_{abs}^a (nm)	ϵ^a (L mol ⁻¹ cm ⁻¹)	λ_{em}^a (nm)	$\phi^{a,b}$	λ_{film} (nm)	E^{ox} [V vs. Fe] ^c	E^{red} [V vs. Fe] ^d
9	349	2500	415	0.33	405	+1.03	-2.67 ^e
11	345	2150	412	0.01	—	+1.17	-2.64
DBPO ²¹	332	2900	366	0.042	—	—	-2.35 ^c
DBPAuCl ²¹	333	—	366	0.134	—	—	-2.26 ^{f,c}

^a Measured in dichloromethane. ^b Measured relative to quinine sulfate (H₂SO₄, 0.1 M), $\phi = 0.55$. ^c All potentials were obtained during cyclic voltammetric investigations in 0.2 M Bu₄NPF₆ in CH₂Cl₂. The platinum electrode diameter: 1 mm, sweep rate: 200 mV s⁻¹. All potentials are referenced to the reversible formal potential of ferrocene/ferrocenium. ^d All potentials were obtained during cyclic voltammetric investigations in 0.1 M Bu₄NPF₆ in THF. Platinum electrode diameter 1 mm, sweep rate: 200 mV s⁻¹. All potentials are referenced to the reversible formal potential of ferrocene/ferrocenium. ^e Quasi-reversible. ^f E_{pc} .

the phosphole ring. The optical properties of the calixphosphole derivatives **9** and **11** were investigated by means of electronic absorption and fluorescence spectroscopy in dichloromethane. Their absorption spectra exhibit both a broad π - π^* transition with a moderate extinction coefficient at 345 and 349 nm, respectively (Fig. 8 and Table 2). The observed bands are characteristic of P-bridged biphenyl derivatives,²¹ and as expected, an analogous band could not be detected for the phosphine complex **4** (Fig. S3†). We further noted that the absorption bands are red-shifted compared to those of 5-phenyldibenzophosphole oxide (DBPO) (Fig. 7) taken as a reference (**9**, $\Delta\lambda = 13$ nm; **11**, $\Delta\lambda = 17$ nm), thus revealing that the presence of the calixarene core induces a decrease of the HOMO-LUMO gap.

Phosphole oxide **9** and gold complex **11** display similar fluorescence spectra (Fig. 8) with emission maxima centered at 412 and 415 nm, respectively. In both cases, the excitation

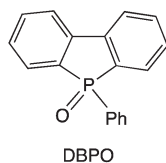
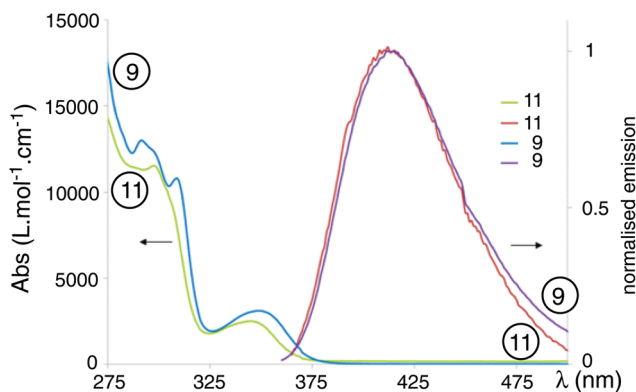


Fig. 7 Structure of DBPO.

Fig. 8 Electronic absorption (blue and green) and emission (violet and red) spectra of compounds **9** and **11** in dilute CH₂Cl₂ solutions.

spectra are similar to the absorption spectra (Fig. S1 and S2†) and the Stokes shifts are moderate (**9**, $\Delta\bar{\nu} = 4557$ cm⁻¹; **11**, $\Delta\bar{\nu} = 4714$ cm⁻¹), suggesting some rearrangement of these molecules upon photoexcitation. As for the absorption properties, fluorescence arises from the dibenzophosphole core (note that the phosphine complex **4** shows no luminescence) and the emission maxima are red-shifted compared to those of the DBPO (**9**, $\Delta\lambda_{\text{em}} = 46$ nm; **11**, $\Delta\lambda_{\text{em}} = 49$ nm). The fluorescence quantum yield measured for complex **11** is lower ($\phi = 0.01$) than that measured for phosphole oxide **9**, which turned out to be an efficient fluorophore ($\phi = 0.33$). Compound **9** also emits as a thin film and the solid-state photoluminescence is almost superimposable on that of the solution (Fig. S1†). This latter observation is consistent with the absence of π -stacking interactions in the solid state (see Fig. 2).

Cyclic voltammetry was further used to study the redox properties of **9** and **11** (Table 2). Both compounds display an irreversible oxidation wave at +1.03 V and +1.17 V, respectively. A quasi-reversible reduction can be seen at -2.67 V for **9**, while the reduction of compound **11** (-2.64 V) is irreversible. Note that no reduction was observed for the phosphine complex **4**. These data, when compared to those of DBPO and DBPAuCl (Table 2), indicate that **9** and **11** are easier to oxidise and more difficult to reduce than the two reference compounds, thus reflecting the electron-donating behaviour of the calixarene core towards the dibenzophosphole unit.

Conclusions

Thermal treatment of the new calixarene-based biarylphosphine **3** in the presence of catalytic amounts of palladium results in two separable, calixarene-fused phospholes with directionally rigid P lone pairs. With the sterically encumbered *endo*-P-calixarene **8**, metal complexes are formed in which the metal centre sits very close to the calixarenyl substituent, thereby creating binding interactions with just one methylene ArCH atom of the calixarene core. The dibenzophosphole complex [Rh(acac)(CO)(**8**)] efficiently catalyses the hydroformylation of styrene with the production of high proportions of branched aldehyde, reflecting the steric effect of the adjacent cavity which may pass through various weak interactions. Ligand **8** is the first example of a calix[4]arene integrating a

phosphole functionality into the cavity wall. As revealed by photophysical and electrochemical studies, the calixarene moiety behaves as an electron donating group with respect to the phosphole unit, endowing it with unique properties compared to known systems. In particular, **9** turned out to be an efficient fluorophore both in solution and in the solid state. Future work will aim at exploiting such molecules as sensors.

Experimental section

General methods

All manipulations were performed in Schlenk-type flasks under dry argon. Solvents were dried by conventional methods and distilled immediately prior to use. CDCl_3 was passed down a 5 cm thick alumina column and stored under nitrogen over molecular sieves (4 Å). Routine ^1H , $^{13}\text{C}\{^1\text{H}\}$ and $^{31}\text{P}\{^1\text{H}\}$ NMR spectra were recorded with Bruker FT spectrometers (AVANCE 400 and 500). ^1H chemical shifts are referenced to residual protiated solvent signals ($\delta = 7.26$ ppm for CDCl_3 and 7.16 ppm for C_6D_6), ^{13}C chemical shifts are reported relative to deuterated solvent signals ($\delta = 77.16$ ppm for CDCl_3 and 128.06 for C_6D_6) and the ^{31}P NMR spectroscopic data are given relative to external H_3PO_4 . Chemical shifts and coupling constants are reported in ppm and Hz, respectively. Elemental analyses were performed by the Service de Microanalyse, Institut de Chimie, Université de Strasbourg. 5-(2-Bromophenyl)-25,26,27,28-tetrapropoxyxycalix[4]arene (**1**),⁸ $[\text{AuCl}(\text{THT})]$,²² $[\text{PdCl}_2(\text{PhCN})_2]$ ²³ and $[\text{PdCl}(\text{8-mq})_2]$ ²⁴ (8-mqH = 8-methylquinoline) were prepared according to the literature procedures.

General procedure for the hydroformylation experiments

The hydroformylation experiments were carried out in a glass-lined, 100 mL stainless steel autoclave containing a magnetic stirring bar. In a typical run, the autoclave was charged with **12** (2 μmol) and extra **8**, and then closed and flushed twice with vacuum/ N_2 . Toluene (20 mL), vinyl arene (2 mmol) and decane (0.25 mL) were added under N_2 . The autoclave was then pressurised (30 bar, CO/H_2 , 1 : 1 v/v) and heated at 60 °C. At the end of each run, the autoclave was cooled to room temperature before being depressurised slowly. A sample was taken and analysed by GC using a WCOT fused silica column (25 m \times 0.25 mm).

Optical and electrochemical properties

UV-Visible spectra were recorded at room temperature on a SPECORD 205 spectrophotometer. The emission and excitation spectral measurements were recorded on an Edinburgh Instruments FL 920 instrument and corrected for the response of the photomultiplier. Quantum yields were calculated relative to quinine sulfate ($\phi = 0.55$ in 0.1 M H_2SO_4). Electrochemical studies were carried out under argon using an Eco Chemie Autolab PGSTAT 30 potentiostat for cyclic voltammetry with the three-electrode configuration: the working elec-

trode was a platinum disc, the reference electrode was a saturated calomel electrode and the counter-electrode was a platinum wire. All potentials were internally referenced to the ferrocene/ferrocenium couple. For the measurements, concentrations of 10^{-3} M of the electroactive species were used in freshly distilled and degassed dichloromethane and 0.2 M tetrabutylammonium hexafluorophosphate.

[5-(2-Diphenylphosphanyl-phenyl)-25,26,27,28-tetrapropoxyxycalix[4]arene] borane (**2**)

n-Butyllithium (1.6 M in hexane, 0.62 mL, 1.00 mmol) was slowly added to a solution of 5-(2-bromophenyl)-25,26,27,28-tetrapropoxyxycalix[4]arene **1** (0.600 g, 0.80 mmol) in THF (50 mL) at -78 °C. After 0.5 h, ClPPH_2 (0.24 mL, 1.30 mmol) was added and the resulting mixture was stirred at 65 °C for 16 h. The reaction was allowed to reach 0 °C, and then $\text{BH}_3\cdot\text{THF}$ (1 M in 2 mL, 2 mmol THF) was added. After stirring for 5 h at room temperature, the solvent was evaporated under reduced pressure. The crude product was purified by column chromatography (CH_2Cl_2 /petroleum ether, 20 : 80 v/v) to afford **2** as a white solid (0.521 g, yield 75%; $R_f = 0.38$, CH_2Cl_2 /petroleum ether, 20 : 80 v/v). ^1H NMR (CDCl_3 , 400 MHz): $\delta = 7.51\text{--}7.41$ (m, 6H, arom. CH, $\text{P}(\text{BH}_3)\text{Ph}_2$), 7.38–7.32 (m, 5H, arom. CH, $\text{P}(\text{BH}_3)\text{Ph}_2$ and C_6H_4), 7.29–7.19 (m, 2H, arom. CH, C_6H_4), 6.82 (d, 2H, arom. CH, calixarene, $^3J = 6.4$ Hz), 6.72–6.69 (m, 1H, arom. CH, C_6H_4), 6.66 (t, 2H, arom. CH, calixarene, $^3J = 7.4$ Hz), 6.62 (d, 2H, arom. CH, calixarene, $^3J = 7.2$ Hz), 6.40 (s, 3H, arom. CH, calixarene), 5.99 (s, 2H, arom. CH, calixarene), 4.44 and 3.13 (AB spin system, 4H, ArCH_2Ar , $^2J = 13.2$ Hz), 4.27 and 2.83 (AB spin system, 4H, ArCH_2Ar , $^2J = 13.2$ Hz), 3.92 (t, 4H, OCH_2 , $^3J = 7.8$ Hz), 3.74 (t, 2H, OCH_2 , $^3J = 7.2$ Hz), 3.66 (t, 2H, OCH_2 , $^3J = 7.2$ Hz), 1.99–1.85 (m, 8H, CH_2CH_3), 1.09 (t, 3H, CH_2CH_3 , $^3J = 7.6$ Hz), 1.04 (t, 3H, CH_2CH_3 , $^3J = 7.6$ Hz), 0.93 (t, 6H, CH_2CH_3 , $^3J = 7.4$ Hz), 0.84–0.89 (m, 3H, BH_3); $^{13}\text{C}\{^1\text{H}\}$ NMR (CDCl_3 , 125 MHz): $\delta = 157.14$ (s, arom Cq-O), 157.09 (s, arom Cq-O), 135.89–121.85 (arom. C's), 76.95 (s, OCH_2), 76.90 (s, OCH_2), 76.54 (s, OCH_2), 30.99 (s, ArCH_2Ar), 30.74 (s, ArCH_2Ar), 23.43 (CH_2CH_3), 23.09 (CH_2CH_3), 10.69 (CH_2CH_3), 10.61 (CH_2CH_3), 10.08 (CH_2CH_3); $^{31}\text{P}\{^1\text{H}\}$ NMR (CDCl_3 , 162 MHz): $\delta = 21.1$ (br. s, $\text{P}(\text{BH}_3)$) ppm; MS (ESI): $m/z = 889.45$ [$\text{M} + \text{Na}$]⁺ expected isotopic profile; elemental analysis calcd (%) for $\text{C}_{58}\text{H}_{64}\text{O}_4\text{PB}$ ($M_r = 866.91$): C 80.36, H 7.44; found (%): C 80.50, H 7.55.

5-(2-Diphenylphosphanyl-phenyl)-25,26,27,28-tetrapropoxyxycalix[4]arene (**3**)

A solution of [5-(2-phosphanyl-phenyl)-25,26,27,28-tetrapropoxyxycalix[4]arene] borane (0.520 g, 0.60 mmol) in MeOH/toluene (1 : 4 mixture, 15 mL) was refluxed for 5 h. After cooling to room temperature, the solution was evaporated to dryness and the residue was dried overnight under vacuum at 40 °C to afford quantitatively phosphine **3** (0.511 g, yield 100%). ^1H NMR (CDCl_3 , 400 MHz): $\delta = 7.34\text{--}7.28$ (m, 7H, arom. CH, PPh_2 and C_6H_4), 7.24–7.13 (m, 5H, arom. CH, PPh_2 and C_6H_4), 7.00–6.96 (m, 1H, arom. CH, C_6H_4), 6.94–6.90 (m, 1H, arom. CH, C_6H_4), 6.67 (d, 2H, arom. CH, calixarene, $^3J =$

6.9 Hz), 6.62–6.57 (m, 1H, arom. CH, calixarene), 6.56 (s, 2H, arom. CH, calixarene), 6.51 (d, 2H, arom. CH, calixarene, $^3J = 6.6$ Hz), 6.42 (t, 2H, arom. CH, calixarene, $^3J = 7.5$ Hz), 6.24 (d, 2H, arom. CH, calixarene, $^3J = 7.2$ Hz), 4.45 and 3.14 (AB spin system, 4H, ArCH₂Ar, $^2J = 13.2$ Hz), 4.38 and 3.01 (AB spin system, 4H, ArCH₂Ar, $^2J = 13.2$ Hz), 3.88 (t, 2H, OCH₂, $^3J = 7.8$ Hz), 3.82 (t, 6H, OCH₂, $^3J = 7.8$ Hz), 1.99–1.86 (m, 8H, CH₂CH₃), 1.03 (t, 9H, CH₂CH₃, $^3J = 7.5$ Hz), 0.96 (t, 3H, CH₂CH₃, $^3J = 7.2$ Hz); $^{13}\text{C}\{^1\text{H}\}$ NMR (CDCl₃, 125 MHz): $\delta = 156.89$ (s, arom Cq-O), 156.39 (s, arom Cq-O), 156.15 (s, arom Cq-O), 148.79–121.94 (arom. C's), 77.11 (s, OCH₂), 77.05 (s, OCH₂), 31.09 (s, ArCH₂Ar), 31.05 (s, ArCH₂Ar), 23.40 (CH₂CH₃), 10.52 (CH₂CH₃), 10.45 (CH₂CH₃); $^{31}\text{P}\{^1\text{H}\}$ NMR (CDCl₃, 162 MHz): $\delta = -12.4$ (s, PPh₂) ppm; MS (ESI): $m/z = 891.41$ [M + K]⁺ expected isotopic profiles; elemental analysis calcd (%) for C₅₈H₆₁O₄P ($M_r = 853.08$): C 81.66, H 7.21; found (%): C 81.48, H 7.08.

Chlorido [5-(2-diphenylphosphanyl-phenyl)-25,26,27,28-tetrapropoxy-calix[4]arene] gold(i) (4)

A solution of [AuCl(THT)] (0.037 g, 0.17 mmol) in CH₂Cl₂ (25 mL) was added to a stirred solution of 3 (0.100 g, 0.17 mmol) in CH₂Cl₂ (25 mL). After stirring for 0.5 h, the solution was concentrated to ca. 2 mL and *n*-hexane (20 mL) was added. A white precipitate formed, which was separated by filtration and dried under vacuum (0.122 g, yield 96%). ^1H NMR (CDCl₃, 500 MHz): $\delta = 7.58$ –7.56 (m, 2H, arom. CH, PPh₂), 7.49–7.44 (m, 8H, arom. CH, PPh₂), 7.37 (t, 1H, arom. CH, C₆H₄, $^3J = 7.2$ Hz), 7.19 (t, 1H, arom. CH, C₆H₄, $^3J = 7.5$ Hz), 6.97 (d, 2H, arom. CH, calixarene, $^3J = 7.0$ Hz), 6.86–6.82 (m, 1H, arom. CH, C₆H₄), 6.74–6.70 (m, 1H, arom. CH, C₆H₄), 6.71 (t, 2H, arom. CH, calixarene, $^3J = 7.5$ Hz), 6.62 (d, 2H, arom. CH, calixarene, $^3J = 7.0$ Hz), 6.31 (t, 1H, arom. CH, calixarene, $^3J = 7.2$ Hz), 6.26 (d, 2H, arom. CH, calixarene, $^3J = 7.2$ Hz), 5.84 (s, 2H, arom. CH, calixarene), 4.46 and 3.14 (AB spin system, 4H, ArCH₂Ar, $^2J = 13.0$ Hz), 4.39 and 2.97 (AB spin system, 4H, ArCH₂Ar, $^2J = 13.5$ Hz), 4.05–3.96 (m, 4H, OCH₂), 3.90 (t, 2H, OCH₂, $^3J = 6.5$ Hz), 3.69 (t, 2H, OCH₂, $^3J = 7.0$ Hz), 2.02–1.95 (m, 4H, CH₂CH₃), 1.95–1.86 (m, 4H, CH₂CH₃), 1.15 (t, 3H, CH₂CH₃, $^3J = 7.2$ Hz), 1.08 (t, 3H, CH₂CH₃, $^3J = 7.5$ Hz), 0.91 (t, 6H, CH₂CH₃, $^3J = 7.2$ Hz); $^{13}\text{C}\{^1\text{H}\}$ NMR (CDCl₃, 125 MHz): $\delta = 157.66$ (s, arom Cq-O), 156.08 (s, arom Cq-O), 155.63 (s, arom Cq-O), 149.00–121.80 (arom. C's), 77.76 (s, OCH₂), 77.15 (s, OCH₂), 76.61 (s, OCH₂), 31.05 (s, ArCH₂Ar), 30.94 (s, ArCH₂Ar), 23.75 (CH₂CH₃), 23.58 (CH₂CH₃), 23.08 (CH₂CH₃), 11.04 (CH₂CH₃), 10.86 (CH₂CH₃), 10.01 (CH₂CH₃); $^{31}\text{P}\{^1\text{H}\}$ NMR (CDCl₃, 162 MHz): $\delta = 26.9$ (s, PPh₂) ppm; elemental analysis calcd (%) for C₅₈H₆₁O₄PAuCl ($M_r = 1085.50$): C 64.17, H 5.66; found (%): C 64.08, H 5.54.

trans-P,P-Dichlorido-bis[5-(2-diphenylphosphanyl-phenyl)-25,26,27,28-tetrapropoxy-calix[4]arene] palladium(ii) (5)

A solution of [PdCl₂(PhCN)₂] (0.020 g, 0.052 mmol) in CH₂Cl₂ (10 mL) was added to a stirred solution of 3 (0.088 g, 0.103 mmol) in CH₂Cl₂ (10 mL). After stirring for 0.5 h, the solution was concentrated to ca. 2 mL and *n*-hexane (20 mL)

was added. The resulting yellow precipitate was separated by filtration and dried under vacuum (0.072 g, yield 95%). ^1H NMR (C₆D₆, 400 MHz): $\delta = 8.08$ (q, 2H, arom. CH, C₆H₄, $^3J = 6.8$ Hz), 8.00–7.96 (m, 6H, arom. CH, PPh₂), 7.14–7.10 (m, 6H, arom. CH, calixarene), 7.08–7.704 (m, 6H, arom. CH, C₆H₄), 7.04–7.00 (m, 14H, arom. CH, PPh₂), 6.79 (s, 6H, arom. CH, calixarene), 6.71–6.69 (m, 4H, arom. CH, calixarene), 6.63–6.62 (m, 6H, arom. CH, calixarene), 4.56 and 3.17 (AB spin system, 8H, ArCH₂Ar, $^2J = 13.5$ Hz), 4.43 and 3.14 (AB spin system, 8H, ArCH₂Ar, $^2J = 13.5$ Hz), 3.88–3.84 (m, 8H, OCH₂), 3.83–3.78 (m, 8H, OCH₂), 1.99–1.88 (m, 16H, CH₂CH₃), 1.03 (t, 6H, CH₂CH₃, $^3J = 7.5$ Hz), 0.94 (t, 12H, CH₂CH₃, $^3J = 7.5$ Hz), 0.93 (t, 6H, CH₂CH₃, $^3J = 7.5$ Hz); $^{13}\text{C}\{^1\text{H}\}$ NMR (C₆D₆, 125 MHz): $\delta = 157.17$ (s, arom Cq-O), 156.70 (s, arom Cq-O), 156.29 (s, arom Cq-O), 147.25–122.57 (arom. C's), 76.95 (s, OCH₂), 76.86 (s, OCH₂), 31.60 (s, ArCH₂Ar), 31.36 (s, ArCH₂Ar), 23.79 (CH₂CH₃), 23.67 (CH₂CH₃), 23.64 (CH₂CH₃), 10.68 (CH₂CH₃), 10.59 (CH₂CH₃), 10.54 (CH₂CH₃); $^{31}\text{P}\{^1\text{H}\}$ NMR (C₆D₆, 162 MHz): $\delta = 22.3$ (s, PPh₂) ppm; MS (ESI): $m/z = 1903.73$ [M + Na]⁺ expected isotopic profiles; elemental analysis calcd (%) for C₁₁₆H₁₂₂O₈P₂PdCl₂ ($M_r = 1883.48$): C 73.97, H 6.53; found (%): C 74.05, H 6.68.

Synthesis of [5-(P-phenyl-5H-benzo[b]phosphindolyl)-25,26,27,28-tetrapropoxy-calix[4]arene] boranes exo-6 and endo-7

A solution of phosphine 3 (4.000 g, 4.69 mmol) and [Pd(OAc)₂] (0.105 g, 0.47 mmol) in toluene (50 mL) was heated at 110 °C for 24 h. After cooling the solution to room temperature, the solvent was removed under vacuum. The crude product was then dissolved in THF. The solution was cooled to 0 °C before the addition of BH₃·THF (1 M in THF, 18.8 mL, 18.76 mmol). After stirring for 2 h, the solution was evaporated to dryness. The residue was purified by column chromatography (CH₂Cl₂/petroleum ether, 5 : 95 v/v) to afford benzophosphole boranes 6 and 7 as white solids.

Phosphole borane 6

(0.740 g, yield 20%; $R_f = 0.28$, CH₂Cl₂/petroleum ether, 5 : 95 v/v); ^1H NMR (CD₂Cl₂, 400 MHz): $\delta = 7.96$ (d, 1H, arom. CH, C₆H₄, $^3J = 7.6$ Hz), 7.78 (d, 1H, arom. CH, calixarene, $^4J(\text{PH}) = 2.4$ Hz), 7.70–7.60 (m, 4H, arom. CH, P(BH₃)Ph and C₆H₄), 7.43–7.37 (m, 2H, arom. CH, P(BH₃)Ph), 7.34 (dt, 2H, arom. CH, P(BH₃)Ph, $^3J = 7.6$ Hz, $^4J(\text{PH}) = 1.6$ Hz), 7.12–7.08 (m, 2H, arom. CH, calixarene), 6.90 (t, 1H, arom. CH, calixarene, $^3J = 7.4$ Hz), 6.18–6.1 (m, 2H, arom. CH, calixarene), 6.06 (d, 1H, arom. CH, calixarene, $^3J = 7.2$ Hz), 5.87 (d, 1H, arom. CH, calixarene, $^3J = 7.6$ Hz), 5.65 (t, 1H, arom. CH, calixarene, $^3J = 7.6$ Hz), 4.71 (d, 1H, arom. CH, calixarene, $^3J = 7.6$ Hz), 4.55 and 3.33 (AB spin system, 2H, ArCH₂Ar, $^2J = 14.0$ Hz), 4.45 and 3.58 (AB spin system, 2H, ArCH₂Ar, $^2J = 13.6$ Hz), 4.45 and 3.15 (AB spin system, 2H, ArCH₂Ar, $^2J = 13.6$ Hz), 4.39 and 3.07 (AB spin system, 2H, ArCH₂Ar, $^2J = 13.4$ Hz), 4.14–4.09 (m, 2H, OCH₂), 4.01 (t, 2H, OCH₂, $^3J = 8.2$ Hz), 3.68 (t, 2H, OCH₂, $^3J = 7.0$ Hz), 3.66–3.56 (m, 2H, OCH₂), 2.01–1.84 (m, 8H, CH₂CH₃), 1.12 (t, 3H, CH₂CH₃, $^3J = 7.4$ Hz), 1.05 (t, 3H, CH₂CH₃, $^3J =$

7.4 Hz), 0.88 (t, 6H, CH₂CH₃, ³J = 7.4 Hz), 0.90–0.77 (m, 3H, P(BH₃)); ¹³C{¹H} NMR (CD₂Cl₂, 125 MHz): δ = 159.87 (d, arom Cq-O, ³J(CP) = 11.4 Hz), 158.59 (s, arom Cq-O), 155.78 (s, arom Cq-O), 155.68 (s, arom Cq-O), 145.08–121.42 (arom. C's), 77.47 (s, OCH₂), 77.39 (s, OCH₂), 77.14 (s, OCH₂), 77.12 (s, OCH₂), 32.07 (s, ArCH₂Ar), 31.34 (s, ArCH₂Ar), 31.22 (s, ArCH₂Ar), 29.66 (d, ArCH₂Ar, ³J(CP) = 4.1 Hz), 23.97 (CH₂CH₃), 23.48 (CH₂CH₃), 23.31 (CH₂CH₃), 11.12 (CH₂CH₃), 11.05 (CH₂CH₃), 10.04 (CH₂CH₃), 9.86 (CH₂CH₃); ³¹P{¹H} NMR (CD₂Cl₂, 162 MHz): δ = 23.0 (br. s, P-BH₃) ppm; elemental analysis calcd (%) for C₅₂H₅₈O₄PB (M_r = 788.80): C 79.18, H 7.41; found (%): C 79.23, H 7.55.

Phosphole borane 7

(2.219 g, yield 60%; R_f = 0.26, CH₂Cl₂/petroleum ether, 5 : 95 v/v); ¹H NMR (CD₂Cl₂, 500 MHz): δ = 7.91 (d, 1H, arom. CH, C₆H₄, ³J = 8.0 Hz), 7.80 (d, 1H, arom. CH, calixarene, ⁴J(PH) = 2.0 Hz), 7.67–7.59 (m, 4H, arom. CH, P(BH₃)Ph and C₆H₄), 7.49 (dt, 1H, arom. CH, C₆H₄, ³J = 7.5 Hz, ⁴J(PH) = 1.0 Hz), 7.40 (dt, 2H, arom. CH, P(BH₃)Ph, ³J = 7.7 Hz, ⁴J(PH) = 2.0 Hz), 7.36 (dt, 1H, arom. CH, P(BH₃)Ph, ³J = 7.7 Hz, ⁵J(PH) = 4.0 Hz), 7.15 (d, 2H, arom. CH, calixarene, ³J = 7.5 Hz), 6.94 (t, 1H, arom. CH, calixarene, ³J = 7.5 Hz), 6.37 (d, 1H, arom. CH, calixarene, ³J = 7.5 Hz), 6.24–6.15 (m, 3H, arom. CH, calixarene), 6.11 (d, 1H, arom. CH, calixarene, ³J = 7.5 Hz), 6.05 (d, 1H, arom. CH, calixarene, ³J = 7.5 Hz), 4.57 and 3.35 (AB spin system, 2H, ArCH₂Ar, ²J = 13.5 Hz), 4.45 and 3.17 (AB spin system, 2H, ArCH₂Ar, ²J = 14.0 Hz), 4.42 and 3.15 (AB spin system, 2H, ArCH₂Ar, ²J = 13.5 Hz), 4.23 and 3.51 (AB spin system, 2H, ArCH₂Ar, ²J = 13.5 Hz), 4.14–4.05 (m, 2H, OCH₂), 4.02 (t, 2H, OCH₂, ³J = 8.2 Hz), 3.71–3.66 (m, 2H, OCH₂), 3.58 (t, 2H, OCH₂, ³J = 7.0 Hz), 2.87–1.98 (m, 3H, P(BH₃)), 1.98–1.88 (m, 6H, CH₂CH₃), 1.84–1.76 (m, 6H, CH₂CH₃), 1.13 (t, 3H, CH₂CH₃, ³J = 7.5 Hz), 1.02 (t, 3H, CH₂CH₃, ³J = 7.5 Hz), 0.87 (t, 3H, CH₂CH₃, ³J = 7.5 Hz), 0.85 (t, 3H, CH₂CH₃, ³J = 7.5 Hz); ¹³C{¹H} NMR (CD₂Cl₂, 125 MHz): δ = 159.91 (d, arom Cq-O, ³J(CP) = 10.8 Hz), 158.53 (s, arom Cq-O), 155.60 (s, arom Cq-O), 155.48 (s, arom Cq-O), 143.98–121.48 (arom. C's), 77.46 (s, OCH₂), 77.32 (s, OCH₂), 77.12 (s, OCH₂), 77.05 (s, OCH₂), 31.87 (s, ArCH₂Ar), 31.30 (s, ArCH₂Ar), 31.18 (s, ArCH₂Ar), 29.73 (d, ArCH₂Ar, ³J(CP) = 4.9 Hz), 23.96 (CH₂CH₃), 23.86 (CH₂CH₃), 23.43 (CH₂CH₃), 23.35 (CH₂CH₃), 11.11 (CH₂CH₃), 10.92 (CH₂CH₃), 9.98 (CH₂CH₃), 9.95 (CH₂CH₃); ³¹P{¹H} NMR (CD₂Cl₂, 162 MHz): δ = 23.3 (br. s, P-BH₃) ppm; MS (ESI): m/z = 827.39 [M + K]⁺ expected isotopic profile; elemental analysis calcd (%) for C₅₂H₅₈O₄PB (M_r = 788.80): C 79.18, H 7.41; found (%): C 79.27, H 7.58.

Phosphole 8

A solution of phosphole borane 7 (2.000 g, 2.53 mmol) in MeOH/toluene (1 : 4 mixture, 15 mL) was heated at 40 °C for 5 h. After cooling to room temperature, the solution was evaporated to dryness and the residue was dried overnight under vacuum to afford quantitatively benzophosphole 8 (1.964 g, yield 100%). ¹H NMR (CDCl₃, 400 MHz): δ = 7.86 (d, 1H, arom. CH, C₆H₄, ³J = 7.6 Hz), 7.69 (s, 1H, arom. CH, calixarene),

7.66–7.63 (m, 1H, arom. CH, C₆H₄), 7.41 (t, 1H, arom. CH, C₆H₄, ³J = 7.6 Hz), 7.42 (t, 2H, arom. CH, PPh, ³J = 7.6 Hz), 7.33–7.28 (m, 3H, arom. CH, PPh), 7.22–7.18 (m, 1H, arom. CH, C₆H₄), 7.04 (d, 2H, arom. CH, calixarene, ³J = 7.6 Hz), 6.79 (t, 1H, arom. CH, calixarene, ³J = 7.2 Hz), 6.51 (d, 1H, arom. CH, calixarene, ³J = 7.2 Hz), 6.31–6.26 (m, 3H, arom. CH, calixarene), 6.23–6.20 (m, 2H, arom. CH, calixarene), 4.60 and 3.34 (AB spin system, 2H, ArCH₂Ar, ²J = 13.2 Hz), 4.49 and 3.19 (AB spin system, 2H, ArCH₂Ar, ²J = 12.8 Hz), 4.46 and 3.17 (AB spin system, 2H, ArCH₂Ar, ²J = 13.2 Hz), 4.35 and 3.52 (AB spin system, 2H, ArCH₂Ar, ²J = 13.6 Hz), 4.05 (t, 2H, OCH₂, ³J = 8.4 Hz), 4.02 (t, 2H, OCH₂, ³J = 8.8 Hz), 3.76 (t, 2H, OCH₂, ³J = 6.6 Hz), 3.71–3.61 (m, 2H, OCH₂), 2.02–1.81 (m, 8H, CH₂CH₃), 1.20–0.77 (m, 3H, P(BH₃)), 1.13 (t, 3H, CH₂CH₃, ³J = 7.6 Hz), 1.05 (t, 3H, CH₂CH₃, ³J = 7.6 Hz), 0.92 (t, 6H, CH₂CH₃, ³J = 7.5 Hz); ¹³C{¹H} NMR (CDCl₃, 101 MHz): δ = 157.98 (s, arom Cq-O), 157.80 (d, arom Cq-O, ³J(CP) = 5.9 Hz), 155.53 (s, arom Cq-O), 155.21 (s, arom Cq-O), 144.08–120.88 (arom. C's), 77.09 (s, OCH₂), 76.97 (s, OCH₂), 76.91 (s, OCH₂), 76.61 (s, OCH₂), 31.58 (s, ArCH₂Ar), 31.19 (s, ArCH₂Ar), 30.30 (d, ArCH₂Ar, ³J(CP) = 8.1 Hz), 23.68 (CH₂CH₃), 23.53 (CH₂CH₃), 23.24 (CH₂CH₃), 23.17 (CH₂CH₃), 10.95 (CH₂CH₃), 10.78 (CH₂CH₃), 10.14 (CH₂CH₃), 10.06 (CH₂CH₃); ³¹P{¹H} NMR (CDCl₃, 162 MHz): δ = -11.5 (s, PPh) ppm; MS (ESI): m/z = 797.37 [M + Na]⁺ expected isotopic profiles; elemental analysis calcd (%) for C₅₂H₅₅O₄P (M_r = 774.97): C 80.59, H 7.15; found (%): C 80.72, H 7.32.

Phosphole oxide 9

To a solution of phosphole 8 (0.050 g, 0.06 mmol) in CH₂Cl₂ (10 mL) was added dropwise H₂O₂ (30% in water, 2.00 mL, 2.50 mmol). The solution was stirred at room temperature for 1 h, and then treated with a mixture of CH₂Cl₂ (10 mL) and water (20 mL). The aqueous layer was separated and washed with CH₂Cl₂ (2 × 10 mL). The organic phases were combined and washed with water (2 × 10 mL). After drying over Na₂SO₄, the solution was filtered through a glass frit before being evaporated to dryness to afford phosphole oxide 9 as a white solid (0.050 g, yield 98%). ¹H NMR (CDCl₃, 500 MHz): δ = 7.81–7.73 (m, 3H, arom. CH, C₆H₄ and P(O)Ph), 7.66 (t, 1H, arom. CH, C₆H₄, ³J = 8.5 Hz), 7.62 (d, 1H, arom. CH, calixarene, ⁴J(PH) = 4.0 Hz), 7.55 (t, 1H, arom. CH, C₆H₄, ³J = 8.0 Hz), 7.53 (t, 1H, arom. CH, P(O)Ph, ³J = 8.0 Hz), 7.44 (dt, 2H, arom. CH, P(O)Ph, ³J = 7.5 Hz, ⁴J(PH) = 3.0 Hz), 7.30 (dt, 1H, arom. CH, C₆H₄, ³J = 7.5 Hz, ⁴J(PH) = 3.5 Hz), 7.14 (d, 2H, arom. CH, calixarene, ³J = 7.0 Hz), 6.94 (t, 1H, arom. CH, calixarene, ³J = 7.2 Hz), 6.71 (d, 1H, arom. CH, calixarene, ³J = 7.5 Hz), 6.27 (t, 1H, arom. CH, calixarene, ³J = 7.5 Hz), 6.22 (t, 1H, arom. CH, calixarene, ³J = 7.5 Hz), 6.14–6.07 (m, 3H, arom. CH, calixarene), 4.55 and 3.29 (AB spin system, 2H, ArCH₂Ar, ²J = 13.0 Hz), 4.44 and 3.16 (AB spin system, 2H, ArCH₂Ar, ²J = 13.0 Hz), 4.41 and 3.14 (AB spin system, 2H, ArCH₂Ar, ²J = 13.5 Hz), 4.16 and 3.60 (AB spin system, 2H, ArCH₂Ar, ²J = 13.0 Hz), 4.11–4.05 (m, 1H, OCH₂), 4.04–3.98 (m, 3H, OCH₂), 3.71–3.66 (m, 2H, OCH₂), 3.58–3.53 (m, 2H, OCH₂), 2.00–1.87 (m, 6H, CH₂CH₃), 1.82–1.75 (m, 2H, CH₂CH₃), 1.12 (t, 3H, CH₂CH₃, ³J = 7.5 Hz), 1.01 (t, 3H,

CH_2CH_3 , $^3J = 7.5$ Hz), 0.88 (t, 3H, CH_2CH_3 , $^3J = 7.5$ Hz), 0.86 (t, 3H, CH_2CH_3 , $^3J = 7.5$ Hz); $^{13}\text{C}\{^1\text{H}\}$ NMR (CDCl_3 , 101 MHz): $\delta = 160.10$ (d, arom Cq-O, $^3J(\text{CP}) = 10.4$ Hz), 158.11 (s, arom Cq-O), 155.11 (s, arom Cq-O), 15.507 (s, arom Cq-O), 142.98–120.58 (arom. C's), 77.13 (s, OCH_2), 76.92 (s, OCH_2), 76.88 (s, OCH_2), 76.62 (s, OCH_2), 31.61 (s, ArCH_2Ar), 31.16 (s, ArCH_2Ar), 30.98 (s, ArCH_2Ar), 28.55 (d, ArCH_2Ar , $^3J(\text{CP}) = 3.1$ Hz), 23.68 (CH_2CH_3), 23.58 (CH_2CH_3), 23.18 (CH_2CH_3), 23.09 (CH_2CH_3), 11.01 (CH_2CH_3), 10.86 (CH_2CH_3), 9.93 (CH_2CH_3); $^{31}\text{P}\{^1\text{H}\}$ NMR (CDCl_3 , 162 MHz): $\delta = 33.4$ (s, $\text{P}(\text{O})\text{Ph}$) ppm; elemental analysis calcd (%) for $\text{C}_{52}\text{H}_{55}\text{O}_5\text{P}$ ($M_r = 790.97$): C 78.96, H 7.01; found (%): C 79.04, H 7.11.

Palladium complex 10

A solution of $[\text{Pd}(\text{8-mq})\text{Cl}]_2$ (0.018 g, 0.03 mmol) in CH_2Cl_2 (10 mL) was added to a stirred solution of **8** (0.049 g, 0.06 mmol) in CH_2Cl_2 (10 mL). After stirring at room temperature for 0.5 h, the reaction mixture was concentrated to about 2 mL and *n*-hexane (20 mL) was added. The yellow precipitate formed was separated by filtration and dried under vacuum (0.050 g, yield 73%). ^1H NMR (CDCl_3 , 500 MHz): $\delta = 9.53$ (tt, 1H, arom. CH of 8-mq, $^3J = 3.5$ Hz, $^5J = 1.0$ Hz), 8.14 (dd, 1H, arom. CH of 8-mq, $^3J = 8.5$ Hz, $^4J = 1.0$ Hz), 7.90 (t, 1H, arom. CH, C_6H_4 , $^3J = 8.2$ Hz), 7.86–7.80 (m, 3H, arom. CH, PPh and Pd-8-mq), 7.77 (d, 1H, arom. CH, calixarene, $^4J(\text{PH}) = 2.0$ Hz), 7.52–7.47 (m, 2H, arom. CH, PPh), 7.38–7.32 (m, 6H, arom. CH, C_6H_4 and CH of 8-mq), 7.26–7.24 (m, 1H, arom. CH of 8-mq), 7.09 (dd, 1H, arom. CH, calixarene, $^3J = 7.5$ Hz, $^4J = 1.5$ Hz), 7.02 (dd, 1H, arom. CH, calixarene, $^3J = 7.5$ Hz, $^4J = 1.5$ Hz), 6.87 (t, 1H, arom. CH, calixarene, $^3J = 7.5$ Hz), 6.75 (d, 1H, arom. CH, calixarene, $^3J = 7.5$ Hz), 6.14–6.13 (m, 2H, arom. CH, calixarene), 6.02–6.01 (m, 1H, arom. CH, calixarene), 5.63 (d, 1H, arom. CH, calixarene, $^3J = 7.5$ Hz), 4.99 (t, 1H, arom. CH, calixarene, $^3J = 7.5$ Hz), 4.60 and 3.35 (AB spin system, 2H, ArCH_2Ar , $^2J = 13.5$ Hz), 4.52 and 4.35 (AB spin system, 2H, ArCH_2Ar , $^2J = 14.0$ Hz), 4.43 and 3.13 (AB spin system, 2H, ArCH_2Ar , $^2J = 13.5$ Hz), 4.33 and 2.98 (AB spin system, 2H, ArCH_2Ar , $^2J = 13.5$ Hz), 4.18–4.08 (m, 2H, OCH_2), 4.03–3.93 (m, 2H, OCH_2), 3.73–3.66 (m, 2H, OCH_2), 3.63–3.59 (m, 1H, OCH_2), 3.48–3.44 (m, 1H, OCH_2), 3.12 and 2.42 (ABX spin system with X = P, 2H, CH_2Pd , $^2J(\text{AB}) = 14.5$ Hz, $^3J(\text{AX}) = 0$ Hz, $^3J(\text{BX}) = 7.5$ Hz), 2.02–1.85 (m, 6H, CH_2CH_3), 1.80–1.73 (m, 2H, CH_2CH_3), 1.13 (t, 3H, CH_2CH_3 , $^3J = 7.2$ Hz), 1.02 (t, 3H, CH_2CH_3 , $^3J = 7.5$ Hz), 0.89 (t, 3H, CH_2CH_3 , $^3J = 7.7$ Hz), 0.85 (t, 3H, CH_2CH_3 , $^3J = 7.5$ Hz); $^{13}\text{C}\{^1\text{H}\}$ NMR (CDCl_3 , 125 MHz): $\delta = 159.74$ (d, arom Cq-O, $^3J(\text{CP}) = 11.1$ Hz), 158.33 (s, arom Cq-O), 155.27 (s, arom Cq-O), 154.80 (s, arom Cq-O), 152.07–120.73 (arom. C's), 77.03 (s, OCH_2), 76.90 (s, OCH_2), 76.85 (s, OCH_2), 76.71 (s, OCH_2), 33.14 (d, Pd- CH_2 , $^2J(\text{CP}) = 3.0$ Hz), 31.82 (s, ArCH_2Ar), 31.15 (s, ArCH_2Ar), 30.92 (s, ArCH_2Ar), 30.58 (d, ArCH_2Ar , $^3J(\text{CP}) = 6.5$ Hz), 23.71 (CH_2CH_3), 23.68 (CH_2CH_3), 23.14 (CH_2CH_3), 23.07 (CH_2CH_3), 11.05 (CH_2CH_3), 10.91 (CH_2CH_3), 10.10 (CH_2CH_3), 9.95 (CH_2CH_3); $^{31}\text{P}\{^1\text{H}\}$ NMR (CDCl_3 , 162 MHz): $\delta = 25.73$ (s, PPh) ppm; MS (ESI): $m/z = 1022.3564$ $[\text{M} - \text{Cl}]^+$ expected isotopic profile.

Gold complex 11

A solution of $[\text{AuCl}(\text{THT})]$ (0.041 g, 0.13 mmol) in CH_2Cl_2 (25 mL) was added to a stirred solution of benzophosphole **8** (0.100 g, 0.13 mmol) in CH_2Cl_2 (25 mL). After stirring at room temperature for 0.5 h, the reaction mixture was concentrated to about 2 mL and then *n*-hexane (20 mL) was added. A white precipitate formed, which was then separated by filtration and dried under vacuum to give complex **11** (0.123 g, yield 95%). ^1H NMR (CDCl_3 , 500 MHz): $\delta = 7.89$ (d, 1H, arom. CH, C_6H_4 , $^3J = 6.0$ Hz), 7.76 (d, 1H, arom. CH, calixarene, $^4J(\text{PH}) = 3.0$ Hz), 7.66–7.61 (m, 3H, arom. CH, C_6H_4 and PPh), 7.58 (t, 1H, arom. CH, PPh, $^3J = 7.7$ Hz), 7.54 (m, 1H, arom. CH, C_6H_4), 7.43 (dt, 2H, arom. CH, PPh, $^3J = 7.7$ Hz, $^4J(\text{PH}) = 2.0$ Hz), 7.35 (dt, 1H, arom. CH, C_6H_4 , $^3J = 7.2$ Hz, $^4J(\text{PH}) = 3.5$ Hz), 7.14 (d, 1H, arom. CH, calixarene, $^3J = 7.0$ Hz), 7.12 (d, 1H, arom. CH, calixarene, $^3J = 7.0$ Hz), 6.93 (t, 1H, arom. CH, calixarene, $^3J = 7.5$ Hz), 6.70 (d, 1H, arom. CH, calixarene, $^3J = 7.0$ Hz), 6.26 (t, 1H, arom. CH, calixarene, $^3J = 7.5$ Hz), 6.25 (t, 1H, arom. CH, calixarene, $^3J = 7.5$ Hz), 6.14 (d, 1H, arom. CH, calixarene, $^3J = 6.2$ Hz), 6.12 (d, 1H, arom. CH, calixarene, $^3J = 6.2$ Hz), 6.08 (d, 1H, arom. CH, calixarene, $^3J = 7.5$ Hz), 4.58 and 3.35 (AB spin system, 2H, ArCH_2Ar , $^2J = 14.0$ Hz), 4.45 and 3.17 (AB spin system, 2H, ArCH_2Ar , $^2J = 13.0$ Hz), 4.40 and 3.15 (AB spin system, 2H, ArCH_2Ar , $^2J = 13.5$ Hz), 4.23 and 3.66 (AB spin system, 2H, ArCH_2Ar , $^2J = 14.0$ Hz), 4.11–4.02 (m, 2H, OCH_2), 4.00 (t, 2H, OCH_2 , $^3J = 8.2$ Hz), 3.74–3.67 (m, 2H, OCH_2), 3.60 (t, 2H, OCH_2 , $^3J = 6.7$ Hz), 1.99–1.85 (m, 6H, CH_2CH_3), 1.82–1.75 (m, 2H, CH_2CH_3), 1.12 (t, 3H, CH_2CH_3 , $^3J = 7.5$ Hz), 1.03 (t, 3H, CH_2CH_3 , $^3J = 7.2$ Hz), 0.87 (t, 3H, CH_2CH_3 , $^3J = 7.5$ Hz), 0.84 (t, 3H, CH_2CH_3 , $^3J = 7.5$ Hz); $^{13}\text{C}\{^1\text{H}\}$ NMR (CDCl_3 , 125 MHz): $\delta = 157.95$ (d, arom Cq-O, $^3J(\text{CP}) = 11.7$ Hz), 157.15 (s, arom Cq-O), 154.21 (s, arom Cq-O), 153.73 (s, arom Cq-O), 142.41–120.37 (arom. C's), 76.09 (s, OCH_2), 75.92 (s, OCH_2), 75.89 (s, OCH_2), 75.71 (s, OCH_2), 30.75 (s, ArCH_2Ar), 30.12 (s, ArCH_2Ar), 30.05 (s, ArCH_2Ar), 28.71 (d, ArCH_2Ar , $^3J(\text{CP}) = 7.1$ Hz), 22.66 (CH_2CH_3), 22.56 (CH_2CH_3), 22.12 (CH_2CH_3), 22.07 (CH_2CH_3), 10.00 (CH_2CH_3), 9.84 (CH_2CH_3), 8.95 (CH_2CH_3), 8.92 (CH_2CH_3); $^{31}\text{P}\{^1\text{H}\}$ NMR (CDCl_3 , 162 MHz): $\delta = -22.8$ (s, PPh) ppm; MS (ESI): $m/z = 1029.31$ $[\text{M} + \text{Na}]^+$ expected isotopic profile; elemental analysis calcd (%) for $\text{C}_{52}\text{H}_{55}\text{AuClO}_4\text{P}$ ($M_r = 1007.39$): C 62.00, H 5.50; found (%): C 62.05, H 5.53.

Rhodium complex 12

A solution of $[\text{Rh}(\text{acac})(\text{CO})_2]$ (0.040 g, 0.15 mmol) in CH_2Cl_2 (15 mL) was added to a stirred solution of benzophosphole **8** (0.120 g, 0.15 mmol) in CH_2Cl_2 (15 mL). After stirring at room temperature for 0.5 h, the solution was concentrated to about 2 mL and MeOH (5 mL) was added. A yellow precipitate formed, which was separated by filtration and then dried under vacuum (0.081 g, yield 52%). ^1H NMR (C_6D_6 , 500 MHz): $\delta = 8.00$ –7.95 (m, 2H, arom. CH, PPh), 7.81 (t, 1H, arom. CH, C_6H_4 , $^3J = 8.0$ Hz), 7.71 (d, 1H, arom. CH, calixarene, $^3J = 7.5$ Hz), 7.68 (d, 1H, arom. CH, calixarene, $^4J(\text{PH}) = 1.5$ Hz), 7.62 (d, 1H, arom. CH, calixarene, $^3J = 7.5$ Hz), 7.20–7.16 (m,

1H, arom. CH, calixarene), 7.16–7.11 (m, 1H, arom. CH, C₆H₄), 7.07 (dd, 1H, arom. CH, C₆H₄, ³J = 7.5 Hz, ⁴J(PH) = 1.5 Hz), 7.01–6.96 (m, 4H, arom. CH of PPh, calixarene and C₆H₄), 6.92 (td, 1H, arom. CH, PPh, ³J = 7.0 Hz, ⁵J(PH) = 1.0 Hz), 6.47 (t, 1H, arom. CH, calixarene, ³J = 7.7 Hz), 6.35–6.30 (m, 2H, arom. CH, calixarene), 6.26 (d, 2H, arom. CH, calixarene, ³J = 7.5 Hz), 5.17 (s, 1H, CH, acac), 4.77 and 4.55 (AB spin system, 2H, ArCH₂Ar, ²J = 13.5 Hz), 4.67 and 3.31 (AB spin system, 2H, ArCH₂Ar, ²J = 13.7 Hz), 4.55 and 3.17 (AB spin system, 2H, ArCH₂Ar, ²J = 13.5 Hz), 4.52 and 3.12 (AB spin system, 2H, ArCH₂Ar, ²J = 13.5 Hz), 4.34–4.24 (m, 2H, OCH₂), 4.15–4.05 (m, 2H, OCH₂), 3.64–3.57 (m, 2H, OCH₂), 3.52–3.44 (m, 2H, OCH₂), 2.19–2.10 (m, 2H, CH₂CH₃), 2.05–1.97 (m, 2H, CH₂CH₃), 1.81–1.72 (m, 2H, CH₂CH₃), 1.76 (s, 3H, CH₃, acac), 1.54–1.56 (m, 2H, CH₂CH₃), 1.51 (s, 3H, CH₃, acac), 1.02 (t, 3H, CH₂CH₃, ³J = 7.2 Hz), 0.93 (t, 3H, CH₂CH₃, ³J = 7.5 Hz), 0.84 (t, 3H, CH₂CH₃, ³J = 7.2 Hz), 0.83 (t, 3H, CH₂CH₃, ³J = 7.2 Hz); ¹³C{¹H} NMR (C₆D₆, 125 MHz): δ = 190.32 (dd, ¹J(CRh) = 75.2 Hz, ²J(CP) = 24.9 Hz, CO), 187.88 (s, CO, acac), 184.33 (s, CO, acac), 159.94 (d, arom Cq-O, ³J(CP) = 10.7 Hz), 158.69 (s, arom Cq-O), 155.50 (s, arom Cq-O), 155.34 (s, arom Cq-O), 142.47–120.82 (arom. C's), 100.59 (s, CH, acac), 77.13 (s, OCH₂), 76.97 (s, OCH₂), 76.94 (s, OCH₂), 32.13 (s, ArCH₂Ar), 31.59 (s, ArCH₂Ar), 31.54 (s, ArCH₂Ar), 29.74 (d, ArCH₂Ar, ³J(CP) = 5.3 Hz), 27.40 (d, ³J(CRh) = 5.4 Hz, CH₃, acac), 27.03 (s, CH₃, acac), 23.93 (CH₂CH₃), 23.73 (CH₂CH₃), 23.49 (CH₂CH₃), 22.07 (CH₂CH₃), 11.07 (CH₂CH₃), 10.83 (CH₂CH₃), 10.22 (CH₂CH₃), 10.12 (CH₂CH₃); ³¹P{¹H} NMR (C₆D₆, 121 MHz): δ = 56.0 (d, PPh, ¹J(PRh) = 172 Hz) ppm; IR: ν = 1975 (strong, CO), 1579 (medium s, acac), 1516 (ms, acac) cm⁻¹; elemental analysis calcd (%) for C₅₈H₆₂O₇Prh (M_r = 1004.99): C 69.32, H 6.22; found (%): C 68.36, H 6.02. Despite repeated elemental analyses, the values obtained for the C analysis were not satisfactory.

X-ray crystal structure determination of gold complex 4

Single crystals of **4** suitable for X-ray analysis were obtained by slow diffusion of methanol into a chloroform solution of the complex. Crystal data: C₅₈H₆₁AuClO₄P, M_r = 1085.46 g mol⁻¹, triclinic, space group P $\bar{1}$, *a* = 11.288(5) Å, *b* = 11.576(5) Å, *c* = 20.999(5) Å, α = 87.574(5)°, β = 86.443(5)°, γ = 64.980(5)°, *V* = 2481.3(16) Å³, *Z* = 2, *D* = 1.453 g cm⁻³, μ = 3.097 mm⁻¹, *F*(000) = 1104.0, *T* = 173(2) K. The sample was studied on a Kappa APEX II diffractometer (graphite monochromated Mo-K_α radiation, λ = 0.71073 Å). The data collection (2θ_{max} = 59.8°, omega scan frames by using 0.7° omega rotation and 30 s per frame, range *hkl*: *h* –15,15 *k* –16,16 *l* –29,29) gave 53 983 reflections. The structure was solved using SIR-97,²⁵ which revealed the non-hydrogen atoms of the molecule. After anisotropic refinement, all of the hydrogen atoms were found using a Fourier difference map. The structure was refined using SHELXL97²⁶ by the full-matrix least-squares technique (use of *F*² magnitude; *x*, *y*, *z*, β_{*ij*} for C, O and P atoms; *x*, *y*, *z* in riding mode for H atoms); 590 variables and 14 382 observations with *I* > 2.0σ(*I*); calcd *w* = 1/[σ²(*F*_o²) + (0.0224*P*)² + 1.5095*P*] where *P* =

(*F*_o² + 2*F*_c²)/3, with the resulting *R* = 0.0299, *R*_w = 0.0589 and *S*_w = 1.048, Δρ < 1.810 e Å⁻³. CCDC 1455340.†

X-ray crystal structure determination of phosphole oxide 9

Single crystals of **9** suitable for X-ray analysis were obtained by slow diffusion of methanol into a chloroform solution of the complex. Crystal data: C₅₂H₅₅ClO₅P, M_r = 790.93 g mol⁻¹, cubic, space group *I*2₁3, *a* = 38.0572(4) Å, *b* = 38.0572(4) Å, *c* = 38.0572(4) Å, α = 90°, β = 90°, γ = 90°, *V* = 55 120.2(17) Å³, *Z* = 48, *D* = 1.144 g cm⁻³, μ = 0.880 mm⁻¹, *F*(000) = 20 256, *T* = 173(2) K. The sample was studied on a Kappa APEX II diffractometer (graphite monochromated Mo-K_α radiation, λ = 0.71073 Å). The data collection (2θ_{max} = 133.4°, omega scan frames by using 0.7° omega rotation and 30 s per frame, range *hkl*: *h* –43,28 *k* –44,45 *l* –45,42) gave 161 417 reflections. The structure was solved using SIR-97,²⁵ which revealed the non-hydrogen atoms of the molecule. After anisotropic refinement, all of the hydrogen atoms were found using a Fourier difference map. The structure was refined using SHELXL97²⁶ by the full-matrix least-squares technique (use of *F*² magnitude; *x*, *y*, *z*, β_{*ij*} for C, O and P atoms; *x*, *y*, *z* in riding mode for H atoms); 1074 variables and 16 277 observations with *I* > 2.0σ(*I*); calcd *w* = 1/[σ²(*F*_o²) + (0.0760*P*)² + 11.7206*P*] where *P* = (*F*_o² + 2*F*_c²)/3, with the resulting *R* = 0.0482, *R*_w = 0.1279 and *S*_w = 1.054, Δρ < 0.403 e Å⁻³. CCDC 1455997.†

X-ray crystal structure determination of palladium complex 11

Single crystals of **11** suitable for X-ray analysis were obtained by slow diffusion of methanol into a chloroform solution of the complex. Crystal data: C₆₂H₆₃ClNO₄PPd, M_r = 1058.96 g mol⁻¹, triclinic, space group P $\bar{1}$, *a* = 9.8908(7) Å, *b* = 19.6964(14) Å, *c* = 27.456(2) Å, α = 94.474(2)°, β = 90.746(2)°, γ = 91.791(2)°, *V* = 5329.2(7) Å³, *Z* = 4, *D* = 1.320 g cm⁻³, μ = 0.477 mm⁻¹, *F*(000) = 2208, *T* = 173(2) K. The sample was studied on a Kappa APEX II diffractometer (graphite monochromated Mo-K_α radiation, λ = 0.71073 Å). The data collection (2θ_{max} = 56.1°, omega scan frames by using 0.7° omega rotation and 30 s per frame, range *hkl*: *h* –13,13 *k* –25,25 *l* –36,36) gave 22 333 reflections. The structure was solved using SIR-97,²⁵ which revealed the non-hydrogen atoms of the molecule. After anisotropic refinement, all of the hydrogen atoms were found using a Fourier difference map. The structure was refined using SHELXL97²⁶ by the full-matrix least-squares technique (use of *F*² magnitude; *x*, *y*, *z*, β_{*ij*} for Pd; C, Cl, N, O and P atoms; *x*, *y*, *z* in riding mode for H atoms); 1298 variables and 25 707 observations with *I* > 2.0σ(*I*); calcd *w* = 1/[σ²(*F*_o²) + (0.0537*P*)² + 15.5771*P*] where *P* = (*F*_o² + 2*F*_c²)/3, with the resulting *R* = 0.0782, *R*_w = 0.1776 and *S*_w = 1.060, Δρ < 2.058 e Å⁻³. CCDC 1545341.†

X-ray crystal structure determination of gold complex 12

Single crystals of **12** suitable for X-ray analysis were obtained by slow diffusion of methanol into a chloroform solution of the complex. Crystal data: C₅₂H₅₅AuClO₄P, M_r = 1007.34 g mol⁻¹, monoclinic, space group *P*2₁, *a* = 9.0854(9) Å, *b* = 18.1789(8) Å, *c* = 13.8937(15) Å, β = 99.456(2)°, *V* = 2263.5(4) Å³,

$Z = 2$, $D = 1.478 \text{ mg m}^{-3}$, $\mu = 3.389 \text{ mm}^{-1}$, $F(000) = 1020$, $T = 173(2) \text{ K}$. The sample was studied on a Kappa APEX II diffractometer (graphite monochromated Mo- K_{α} radiation, $\lambda = 0.71073 \text{ \AA}$). The data collection ($2\theta_{\text{max}} = 5.8^{\circ}$, omega scan frames by using 0.7° omega rotation and 30 s per frame, range $hkl: h -11,11 k -23,24 l -18,18$) gave 22 333 reflections. The structure was solved using SIR-97,²⁵ which revealed the non-hydrogen atoms of the molecule. After anisotropic refinement, all of the hydrogen atoms were found using a Fourier difference map. The structure was refined using SHELXL97²⁶ by the full-matrix least-squares technique (use of F^2 magnitude; x, y, z, β_{ij} for Au; C, Cl, O and P atoms; x, y, z in riding mode for H atoms); 531 variables and 10 857 observations with $I > 2.0\sigma(I)$; $\text{calcd } w = 1/[\sigma^2(F_o^2)]$, with the resulting $R = 0.0497$, $R_w = 0.0825$ and $S_w = 1.023$, $\Delta\rho < 2.370 \text{ e \AA}^{-3}$. CCDC 1545342.†

Computational details

Calculations were performed using the ADF 2013 software package.²⁷ Slater type orbitals were used with all-electron double- ζ quality basis sets at the DFT level with the B3LYP functional.²⁸ Dispersive interactions were taken into account through recent Grimme corrections with a damping function.²⁹ Scalar relativistic effects were included through ZORA Hamiltonians.³⁰ Full geometry optimization was performed on each structure. The NMR shielding of the protons of the methylene groups was computed using ADF NMR modules. Single point calculations using the Gaussian 09 software package³¹ were done at the DFT level with the B3LYP functional on the ADF optimized structure in order to compute wavefunctions suitable for topological analyses. The atoms were described using the def2-SV basis sets on all atoms³² and the associated pseudopotentials for Rh, Pd and Au cations.³³ Weak interactions were studied through NCI analysis of the Gaussian wavefunction.³⁴

References

- (a) C. Wieser, C. B. Dieleman and D. Matt, *Coord. Chem. Rev.*, 1997, **165**, 93–161; (b) S. Steyer, C. Jeunesse, D. Armspach, D. Matt and J. Harrowfield, in *Calixarenes*, ed. Z. Asfari, V. Böhmer, J. Harrowfield and J. Vicens, 2001, pp. 513–535; (c) D. M. Homden and C. Redshaw, *Chem. Rev.*, 2008, **108**, 5086–5130; (d) C. J. Copley and P. G. Pringle, *Catal. Sci. Technol.*, 2011, **1**, 239–242; (e) A. Marson, P. W. N. M. van Leeuwen and P. C. J. Kamer; (f) D. Sémeril and D. Matt, *Coord. Chem. Rev.*, 2014, **279**, 58–95.
- (a) R. Paciello, L. Siggel and M. Röper, *Angew. Chem., Int. Ed.*, 1999, **38**, 1920–1923; (b) F. J. Parlevliet, C. Kiener, J. Fraanje, K. Goubitz, M. Lutz, A. L. Spek, P. C. J. Kamer and P. W. N. M. van Leeuwen, *J. Chem. Soc., Dalton Trans.*, 2000, 1113–1122; (c) C. Dieleman, S. Steyer, C. Jeunesse and D. Matt, *J. Chem. Soc., Dalton Trans.*, 2001, 2508–2517;
- (d) M. Lejeune, D. Sémeril, C. Jeunesse, D. Matt, F. Peruch, P. L. Lutz and L. Ricard, *Chem. – Eur. J.*, 2004, **10**, 5354–5360; (e) D. Sémeril, C. Jeunesse, D. Matt and L. Toupet, *Angew. Chem., Int. Ed.*, 2006, **45**, 5810–5814; (f) L. Monnereau, D. Sémeril and D. Matt, *Green Chem.*, 2010, **12**, 1670–1673; (g) L. Monnereau, D. Sémeril, D. Matt and L. Toupet, *Chem. – Eur. J.*, 2010, **16**, 9237–9247; (h) L. Monnereau, D. Sémeril and D. Matt, *Chem. Commun.*, 2011, **47**, 6626–6628; (i) M. Jouffroy, R. Gramage-Doria, D. Armspach, D. Sémeril, W. Oberhauser, D. Matt and L. Toupet, *Angew. Chem., Int. Ed.*, 2014, **53**, 3937–3940; (j) M. Jouffroy, D. Armspach, D. Matt, K. Osakada and D. Takeuchi, *Angew. Chem., Int. Ed.*, 2016, **55**, 8367–8370.
- (a) K. Ito, M. P. Schramm, M. Kanaura, M. Ide, N. Endo and T. Iwasawa, *Tetrahedron Lett.*, 2016, **57**, 233–236; (b) M. Kanaura, N. Endo, M. P. Schramm and T. Iwasawa, *Eur. J. Org. Chem.*, 2016, 4970–4975.
- (a) D. Sémeril, C. Jeunesse and D. Matt, *C. R. Chim.*, 2008, **11**, 583–594; (b) N. Khiri, E. Bertrand, M. J. Ondel-Eymin, Y. Rousselin, J. Bayardon, P. D. Harvey and S. Jugé, *Organometallics*, 2010, **29**, 3622–3631; (c) L. Monnereau, D. Sémeril, D. Matt and L. Toupet, *Transition Met. Chem.*, 2013, **38**, 821–825.
- (a) Y. Kuninobu, T. Yoshida and K. Takai, *J. Org. Chem.*, 2011, **76**, 7370–7376; (b) V. Diemer, A. Berthelot, J. Bayardon, S. Jugé, F. R. Leroux and F. Colobert, *J. Org. Chem.*, 2012, **77**, 6117–6127; (c) K. Fourmy, D. H. Nguyen, O. Dechy-Cabaret and M. Gouygou, *Catal. Sci. Technol.*, 2015, **5**, 4289–4323; (d) T. Okada, Y. Unoh, T. Satoh and M. Miura, *Chem. Lett.*, 2015, **44**, 1598–1600.
- F. Elaieb, A. Hedhli, D. Sémeril, D. Matt and J. Harrowfield, *Eur. J. Org. Chem.*, 2016, 3103–3108.
- K. Baba, M. Tobisu and N. Chatani, *Angew. Chem., Int. Ed.*, 2013, **52**, 11892–11895.
- A. Casnati, M. Fochi, P. Minari, A. Pochini, M. Reggiani, R. Ungaro and D. N. Reinhoudt, *Gazz. Chim. Ital.*, 1996, **126**, 99–106.
- C. D. Gutsche, in *Calixarenes, Monographs in Supramolecular Chemistry*, ed. J. F. Stoddart, Royal Society of Chemistry, Cambridge, UK, 1989, p. 111.
- E. Herrero-Gómez, C. Nieto-Oberhuber, S. López, J. Benet-Buchholz and A. M. Echavarren, *Angew. Chem., Int. Ed.*, 2006, **45**, 5455–5459.
- S. Vuoti, M. Haukka and J. Purslainen, *J. Organomet. Chem.*, 2007, **692**, 5044–5052.
- F. Elaieb, A. Hedhli, D. Sémeril and D. Matt, *Eur. J. Org. Chem.*, 2016, 1867–1873.
- Spartan v. 2.0.3*, Wavefunction Inc., Irvine, CA.
- C. A. Tolman, *Chem. Rev.*, 1977, **77**, 313–348.
- L. Falivene, R. Credendino, A. Poater, A. Petta, L. Serra, R. Oliva, V. Scarano and L. Cavallo, *Organometallics*, 2016, **35**, 2286–2293.
- I. Bernal and R. A. Lalancette, *C. R. Chim.*, 2015, **18**, 929–934.
- P. Braunstein, D. Matt, Y. Dusausoy, J. Fischer, A. Mitschler and L. Ricard, *J. Am. Chem. Soc.*, 1981, **103**, 5115–5125.

- 18 (a) P. S. Pregosin, *NMR in Organometallic Chemistry*, Wiley-VCH, Weinheim, Germany, 2012, pp. 251–252; (b) M. Teci, E. Brenner, D. Matt and L. Toupet, *Eur. J. Inorg. Chem.*, 2013, 2841–2848.
- 19 A. Oukhrib, L. Bonnafoux, A. Panossian, S. Waifang, D. H. Nguyen, M. Urrutigoity, F. Colobert, M. Gouygou and F. R. Leroux, *Tetrahedron*, 2014, **70**, 1431–1436.
- 20 M. Montag, I. Efremenko, R. Cohen, G. Leitus, L. J. W. Shimon, Y. Diskin-Posner, Y. Ben-David, J. M. L. Martin and D. Milstein, *Chem. – Eur. J.*, 2008, **14**, 8183–8194.
- 21 H. C. Su, O. Fadhel, C. J. Yang, T. Y. Cho, C. Fave, M. Hissler, C. C. Wu and R. Réau, *J. Am. Chem. Soc.*, 2006, **128**, 983–995.
- 22 R. Usón, A. Laguna and M. Laguna, *Inorg. Synth.*, 1989, **26**, 85–87.
- 23 F. R. Hartley, *The Chemistry of Platinum and Palladium*, Wiley, New York, 1973.
- 24 A. C. Cope and E. C. Friedrich, *J. Am. Chem. Soc.*, 1968, **90**, 909–913.
- 25 A. Altomare, M. C. Burla, M. Camalli, G. Cascarano, C. Giacovazzo, A. Guagliardi, A. G. G. Moliterni and G. Polidori, *J. Appl. Crystallogr.*, 1998, **31**, 74–77.
- 26 G. M. Sheldrick, *SHELXL-97, Program for the Refinement of Crystal Structures*, University of Göttingen, Germany, 1997.
- 27 ADF2013, SCM, Theoretical Chemistry, Vrije Universiteit, Amsterdam, The Netherlands, <http://www.scm.com>.
- 28 P. J. Stephens, F. J. Devlin, C. F. Chabalowski and M. J. Frisch, *J. Phys. Chem.*, 1994, **98**, 11623–11627.
- 29 (a) S. Grimme, J. Antony, S. Ehrlich and H. Krieg, *J. Chem. Phys.*, 2010, **132**, 154104; (b) S. Grimme, S. Ehrlich and L. Goerigk, *J. Comput. Chem.*, 2011, **32**, 1456–1465.
- 30 E. van Lenthe, A. Ehlers and E. J. Baerends, *J. Chem. Phys.*, 1999, **110**, 8943–8953.
- 31 M. J. Frisch, G. W. Trucks, H. B. Schlegel, G. E. Scuseria, M. A. Robb, J. R. Cheeseman, G. Scalmani, V. Barone, B. Mennucci, G. A. Petersson, H. Nakatsuji, M. Caricato, X. Li, H. P. Hratchian, A. F. Izmaylov, J. Bloino, G. Zheng, J. L. Sonnenberg, M. Hada, M. Ehara, K. Toyota, R. Fukuda, J. Hasegawa, M. Ishida, T. Nakajima, Y. Honda, O. Kitao, H. Nakai, T. Vreven, J. A. Montgomery Jr., J. E. Peralta, F. Ogliaro, M. Bearpark, J. J. Heyd, E. Brothers, K. N. Kudin, V. N. Staroverov, R. Kobayashi, J. Normand, K. Raghavachari, A. Rendell, J. C. Burant, S. S. Iyengar, J. Tomasi, M. Cossi, N. Rega, J. M. Millam, M. Klene, J. E. Knox, J. B. Cross, V. Bakken, C. Adamo, J. Jaramillo, R. Gomperts, R. E. Stratmann, O. Yazyev, A. J. Austin, R. Cammi, C. Pomelli, J. W. Ochterski, R. L. Martin, K. Morokuma, V. G. Zakrzewski, G. A. Voth, P. Salvador, J. J. Dannenberg, S. Dapprich, A. D. Daniels, Ö. Farkas, J. B. Foresman, J. V. Ortiz, J. Cioslowski and D. J. Fox, *Gaussian 09, Revision D.01*, Gaussian, Inc., Wallingford CT, 2009.
- 32 A. Schäfer, H. Horn and R. Ahlrichs, *J. Chem. Phys.*, 1992, **97**, 2571–2577.
- 33 K. Eichkorn, F. Weigend, O. Treutler and R. Ahlrichs, *Theor. Chem. Acc.*, 1997, **97**, 119–124.
- 34 J. Contreras-Garcia, E. R. Johnson, S. Keinan, R. Chaudret, J. P. Piquemal, D. N. Beratan and W. T. Yang, *J. Chem. Theor. Comput.*, 2011, **7**, 625–632.